International Journal of Environmental Science and Technology
https://doi.org/10.1007/s13762-024-05858-4

ORIGINAL PAPER

Simultaneous improvement of nanofluid stability and CO_2 absorption by chitosan-grafted multi-walled carbon nanotubes dispersed in MDEA-based nanofluid

S. Sadeddin[1] · M. Abbasi[1] · S. Riahi[1]

Received: 4 December 2023 / Revised: 16 June 2024 / Accepted: 19 June 2024

Abstract
Due to the growing concern over limiting carbon dioxide (CO_2) emissions and combating climate change, the need for innovative measures to mitigate carbon dioxide emissions has become increasingly significant. For the first time, the proposed research affirms the decent functionality of the polymer grafting method in simultaneously prolonging stability and enhancing gas removal capacity. To achieve this, the surface of acid-treated Multi-Walled Carbon Nanotubes was modified using a 1,3-Diaminopropane solution. A straightforward and novel synthesis procedure was utilized to produce chitosan-grafted Multi-Walled Carbon Nanotubes. 10 wt% aqueous MDEA-based nanofluids were prepared, incorporating both chitosan-grafted Multi-Walled Carbon Nanotubes and amine-functionalized Multi-Walled Carbon Nanotubes, to compare CO_2 absorption performance and kinetics at various particle concentrations. Results revealed significant enhancements in CO_2 removal efficiency, absorption rates, and nanofluid stability when chitosan-grafted Multi-Walled Carbon Nanotubes were employed, in contrast to amine-functionalized Multi-Walled Carbon Nanotubes and a neat amine solution. The main focus of this paper was to enhance nanofluid stability, which is one of the key properties of nanofluids in their application for CO_2 absorption. The agglomeration and sedimentation formation in nanofluids containing amine-functionalized MWCNTs was resolved by adding surfactants. This was a short-term solution, while Zeta potential measurements and sediment photography over one month demonstrated long-lasting stability attributed to the incorporation of chitosan chains on the surface of amine-functionalized MWCNTs. Moreover, the addition of chitosan-grafted Multi-Walled Carbon Nanotubes resulted in a 12 and 20% improvement in CO_2 capture capacity compared to amine-functionalized Multi-Walled Carbon Nanotubes and a fresh solvent, respectively.

Keywords Absorption · CO_2 removal · Chitosan · MDEA solution · Nanofluid · Polymer grafted

Introduction

The world is currently grappling with unprecedented shifts in climate patterns, a crisis driven largely by human-induced emissions of greenhouse gases (Figueroa et al. 2008). Despite this impending threat, fossil fuel consumption has continued to raise and is expected to increase by 2% yearly till 2030 (Gür 2022). Fortunately, CO_2 is a Greenhouse Gas (GHG) with an increasing potential for transforming into value-added products, as well as conforming to international emission reduction goals (like the Paris Agreement) (Pahija et al. 2022). Different methods are used to mitigate carbon dioxide concentration in the atmosphere like absorption, adsorption, membrane and cryogenics; among which CO_2 absorption using amine-based solvents is the most commercially, technically and environmentally available separation method throughout the world (Ngoy et al. 2014; Khaheshi et al. 2019). The most widely used Alkanolamines in CO_2 capture processes are Monoethanolamine (MEA), Diethanolamine (DEA), and Methyl diethanolamine (MDEA); each has some advantages and disadvantages (Khodadadi et al. 2019). It is clear that no single solvent shows all positive attributes for CO_2 removal; however, amongst solvent options that were represented above, MDEA has become

Editorial responsibility: L. Yin.

✉ S. Riahi
Riahi@ut.ac.ir

[1] Institute of Petroleum Engineering, School of Chemical Engineering, College of Engineering, University of Tehran, Tehran, Iran

Published online: 09 July 2024

more important due to the higher CO_2 solubility, low vapour loss, better thermal stability, less volatility and low enthalpy of reaction (Weiland et al. 2010).

Recent studies have been focused on the state-of-the-art approach to the separation of CO_2 molecules. This approach introduced solid particles (nanoparticles in particular) into a base fluid like amine solvents. Various types of nanoparticles, such as SiO_2, Al_2O_3, Fe_3O_4, TiO_2 and CNTs are employed for preparing colloidal nanosuspensions. The purpose of using nanosuspensions is to promote absorption rate, absorption capacity and solvent stability as well as decrease solvent vapour pressure and minimize the energy penalty (Krishnamurthy et al. 2006; Agarwal et al. 2010; Nabipour et al. 2017). Fang et al. (2014) reported the CO_2 absorption performance of SiO_2, Al_2O_3, Fe_3O_4 and CNT particles dissolved in water, DEA and MDEA aqueous solutions. Results demonstrated that hydrophilic particles (SiO_2 and Al_2O_3) had better removal performance at higher concentrations (0.1 wt%), while hydrophobic particles (Fe_3O_4 and CNT) performed favourably at lower concentrations (0.02 wt%). Besides, MDEA proved to be a more efficient base solvent for CNT containing nanosuspensions. (Cui et al. 2018) discovered a 2% reduction in CO_2 absorption loading by the addition of porous solids (MWCNTs, silica gel and MCM-41). These porous particles were dissolved in 100 g of a non-aqueous solution containing 30 wt% monoethylethanolamine (EMEA) and 70 wt% diethylethanolamine (DEEA). These solids could also improve desorption performance. Golkhar et al. (2013) employed silica and CNT nanofluids in a hollow fiber membrane contactor to increase CO_2 absorption. MWCNTs containing nanofluids exhibited a better removal performance by increasing separation efficiency up to 40% at low solvent rates and up to 20% at high flow rates. Nabipour et al. (2017) suggested that applying 0.02 wt% carboxylic MWCNTs to Sulfinol-M enhances absorption capacity up to 23.2%. (Saidi 2020) revealed the positive impact of CNT and SiO_2 nanoparticles on CO_2 absorption inside a hollow fiber membrane. 4-diethylamino-2-butanol (DEAB)- water nanofluid was used as the base solvent to separate CO_2 from the CO_2/N_2 mixture. Sensitive analysis confirmed the better performance of CNT nanoparticles.

Nanoscale solid sorbents were then further promoted by the incorporation of different functional groups and polymer chains in novel proposed technologies. This approach was mainly adopted to overcome dispersibility issue in prepared nanofluids and to improve their stability and uniformity (Tsubokawa 2011). Within various captivating characteristics of nanofluids, sustaining stable conditions stands as the foremost fundamental prerequisite in exploring exceptional attributes of nanofluids (Urmi et al. 2020). Poor stable conditions in nanofluids would result in aggregation and sedimentation. This would affect the density and viscosity of nanofluids and hinder the industrial application of nanofluids (Liu et al. 2022). The novel proposed nanosuspensions can also chemically remove CO_2 molecules by the reaction between gas molecules and amine groups in tethered chains. Jorge and Coulombe (2015) prepared three samples of amine-functionalized MWCNTs by either grafting or decomposition of a nitrogen-rich polymeric layer on the surface of home-synthesized MWCNTs. Maximum CO_2 uptake capacity was 36% higher than RO (reverse-osmosis) water, and the stable condition of the MWCNTs in the host fluid was confirmed by the addition of nucleophilic groups. Ha et al. (2022) examined the CO_2 capture performance of four nanofluids containing Fe_3O_4, Fe_3O_4@AA (coated by ascorbic acid), Fe_3O_4@AA@SiO_2 (coated by SiO_2) and Fe_3O_4@AA@SiO_2@NH_2 (amine functionalized by APTES) nanoparticles in the water base fluid. It was proved that the amine-functionalized double shell coated magnetite enhanced the absorption capacity by 59.2% at 0.3 wt% compared to Fe_3O_4, Fe_3O_4@AA and Fe_3O_4@AA@SiO_2. Moreover, Fe_3O_4@AA@SiO_2@NH_2 particles were proved stable in water by DLS (Dynamic light scattering) analysis. Irani et al. (2018) enhanced the CO_2 absorption of aqueous 40 wt% MDEA solution by adding 0.2 wt% PEI-KUST-1 (PEI functionalized /KUST particles). Using Zeta Potential method, the solution was proved stable. Rahimi et al. (2020) experimentally studied the effect of different host fluids on CO_2 removal capacity and nanofluid stability in the presence of hydrophilic and hydrophobic MWCNTs. Results represented higher absorption enhancement of hydrophobic particles (pristine and amine-functionalized MWCNTs) as well as better absorption performance of MDEA in comparison with MEA and mixed amines. Li et al. (2015) examined CO_2 capture enhancement of solvent-free nanofluids with ionically tethered polyether amine terminated polymer in comparison to pristine MWCNTs and tethered polyether amine. They discovered that higher MW, higher ethylene oxide/propylene oxide ratio, and more unprotonated amine and oxygenated groups positively impacted removal capacity and fluid stability during multiple absorption–desorption cycles. Arshadi et al. (2019) modified Fe_3O_4 nanoparticles by employing various organic and inorganic reagents with either hydrophobic or hydrophilic functional groups. Fe_3O_4@SiO_2-SNH_2 particles, amongst other synthesized particles, exhibited a 49.7% increase in CO_2 absorption capacity owing to high symmetric amine functional sites. They also found that at 0.4 wt% concentration of Fe_3O_4@SiO_2-SNH_2, the solution performed optimally. Baghery et al. (2019) measured the CO_2 absorption by amine-functionalized MWCNT particles in pure water as well as 5, 10 and 15 wt% MDEA aqueous solutions. They determined the optimum particle concentration in water-based solvent to be 0.005 wt%. It was reported that absorption capacity could be enhanced up to 26.4% in this mass fraction. Furthermore, the stability issue was solved by adding 0.1 wt% PVA as a dispersant.

Chitosan is a hydrophilic, nature-friendly, and non-toxic polysaccharide with a linear structure that is degradable and compatible from a biological standpoint (Peniche et al. 2003). Other advantages of this biopolymer include being conveniently available, inexpensive, renewable, and environmentally sustainable (Hsan et al. 2020). Chitosan, with a structure rich in amino and hydroxyl groups, proves to be an appealing choice for CO_2 removal operations (Masuko et al. 2005). However, chitosan, itself, due to its low surface area and crystalline structure, cannot serve as a decent CO_2 adsorbent. It can extensively be used to prepare functional derivatives by chemical treatment, grafting, and ionic reaction with a compound that has an amorphous structure and high surface area (Kumar et al. 2017; Hsan et al. 2020). On the other hand, owing to the unique properties of multi-walled carbon nanotubes, including high surface area, hollow tubular structure, and remarkable electrical, mechanical, and thermal properties, they have come to prominence in commercial applications like their incorporation in polymer composites (Spitalsky et al. 2010; Basheer et al. 2020). Nevertheless, MWCNTs are highly hydrophobic and may coalesce in polar media (Breuer and Sundararaj 2004; Vaisman et al. 2006). To overcome this issue, MWCNTs' sidewall can be modified covalently using hydrophilic agents (Breuer and Sundararaj 2004). Oxygen-containing functional groups (e.g., C–O, C=O, O–C=O) can be chemically attached or grafted at the tube ends and also defects on the sidewalls of MWCNTs to tailor the dispersion properties of these particles (Wepasnick et al. 2011). These functional groups also expand the practical utilization of nanostructures (Wepasnick et al. 2010a, b). Carboxylic acid groups can be bonded via strong acid treatments (e.g., H_2SO_4) to enhance the colloidal stability of nanostructures and develop multifunctional features in them to be used in polymer incorporation (Wepasnick et al. 2010a; b; Smith et al. 2009). These treatments can also eliminate amorphous carbon and metallic impurities from as-synthesized MWCNTs (Ismail et al. 2008).

Following the oxidation process, chitosan can be implemented on the surface of MWCNTs by an acid–base reaction between chitosan's primary amine groups and carboxylic groups of oxidized MWCNTs. The resulting product indicates a higher level of absorption capacity owing to the improved pore fields and abundance of amino and hydroxyl groups in polymer chains (Hsan et al. 2020). Besides, the toxicity issue with carboxyl groups, i.e. in acid-treated MWCNTs can be addressed by the attachment of a non-toxic and nature-friendly configuration like chitosan (Hsan et al. 2020).

According to the literature, no study investigates the CO_2 absorption performance of polymer-grafted MWCNTs nanofluids. Over the past years, studies have mostly concentrated on the gas adsorption performance of these particles. This is the first study to undertake a quantitative investigation of the CO_2 absorption performance of polymer-grafted MWCNTs dispersed in an aqueous amine solvent. Moreover, in previous studies, little attention has been paid to the stability problem of colloidal suspension. This study aims to propose an easily applicable method to address this unresolved issue. In this study, chemically reactive sites were developed on acid-treated MWCNTs' surface by introducing amine groups (aMWCNT). Amine-terminated chitosan chains were then tethered on aMWCNTs (gMWCNT). Amine functionalized MWCNTs, and chitosan-grafted MWCNTs were suspended in an aqueous MDEA solution (10 wt%), and their gas removal capacity was measured at various operation temperatures and pressure. Coupling the applications of these state-of-the-art nanoparticles with the well-established amine solvents, can not only enhance CO_2 removal capacity with few changes in existing plants, but also reduce capital costs of gas sweetening units. Furthermore, nanofluid's longevity was extended by the incorporation of chitosan polymer chains on the surface of amine-functionalized MWCNTs.

Materials and Methods

Material

MWCNTs were obtained from Neutrino Nano Company. Sulfuric acid (H_2SO_4, purity: 96%, Merck), nitric acid (HNO_3, purity: 65%, Merck), Ethanol (C_2H_6O, purity: 99.9%, Merck), and 1,3-Diaminopropane ($C_3H_{10}N_2$, purity: 99%, Merck) were used in order to chemically modify and functionalize raw MWCNTs. MDEA (N-methyldiethanolamine) was supplied as a base solvent from Merck Company, Germany. A 10 wt% HCl solution was employed to control and adjust the pH of the solution during the grafting process. CO_2 gas (99.99% purity) was purchased from Raha Gas Company, Iran.

Chemical modification of MWCNTs

Functionalization of crude MWCNT was conducted in three steps:

Hydrophilization step

MWCNTs are inherently hydrophobic. Carboxylic groups were incorporated onto their surface using a concentrated acid solution to introduce chemically reactive sites. This process began by immersing MWCNTs in a mixture of 5 M sulfuric acid and 5 M nitric acid at a 3:1 volume ratio. Subsequently, the suspension underwent one hour of ultrasonic bath sonication to enhance dispersion within the acid

mixture. The mixture was refluxed, washed with distilled water, cooled, and then dried in an oven.

Amine functionalization step

To functionalize the pretreated MWCNTs with amine groups, acid-treated MWCNTs were combined with a 30% weight solution of 1,3-Diaminopropane in ethanol and stirred for 12 h. The mixture was subsequently filtered and dried at 80 °C, resulting in the product referred to as 'aMWCNTs'. A schematic representation of an aMWCNT particle is provided in Fig. 1.

Polymer grafting step

The stability of nanofluids containing amine-functionalized MWCNT particles was traditionally improved by the addition of surfactants. However, in this study, a novel polymer grafting method was employed to enhance the stability of amine-functionalized nanoparticles. Biodegradable, biocompatible, and amino-terminated chitosan was selected as the grafting polymer.

A specific quantity of chitosan was dissolved in a water–ethanol mixture while stirring. Subsequently, amine-functionalized MWCNTs were introduced into the mixture and subjected to reflux at 80°C for 4 h. This process facilitated the bonding of polymer chains to MWCNT particles. After 24 h, the solid was separated from impurities through filtration by multiple washes with an ethanol–water mixture. Finally, the chitosan-grafted MWCNTs were dried in an oven for 30 min. The steps of the grafting process are illustrated in Fig. 2.

Figure 3 illustrates the schematic of a gMWCNT particle. Chitosan grafting was carried out at three different mass fractions (0.025, 0.05, and 0.1 g) of this polymer. Gas absorption capacity was then measured for each sample to determine the one with the highest removal capability.

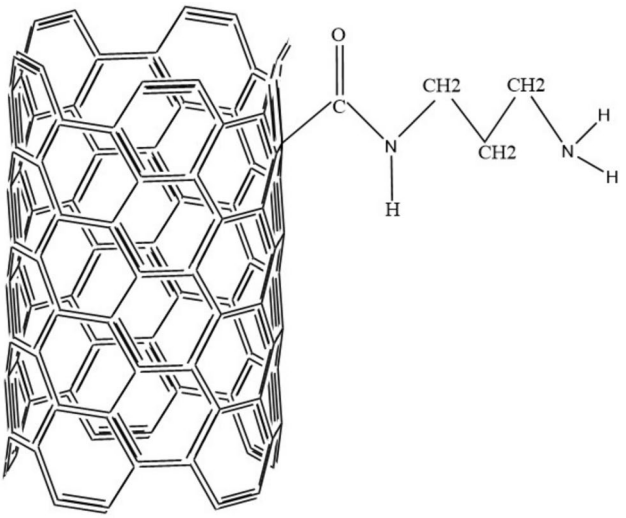

Fig. 1 Schematic representation of the amine-functionalized MWCNTs

Preparation of amine-based nanofluids

The widely used two-step method was employed to disperse Nanoparticles in the host fluid homogeneously (Yu et al. 2019). Pre-synthesized aMWCNT and gMWCNT particles were mixed with aqueous MDEA solution (10 wt%) using ultrasonic mixing technology. Nanofluids were prepared by adding a range of concentrations (0.0005, 0.001, 0.005, 0.01, and 0.02 wt%) of both aMWCNTs and gMWCNTs to the base solvent and subjecting them to sonication for 45 min. No surfactants were added to stabilize the prepared liquid absorbents.

Experimental apparatus for CO_2 absorption

The custom-built apparatus, illustrated in Fig. 4, consists of two vessels connected by pipes. One vessel contains the gas, while the other is used for absorption experiments. The

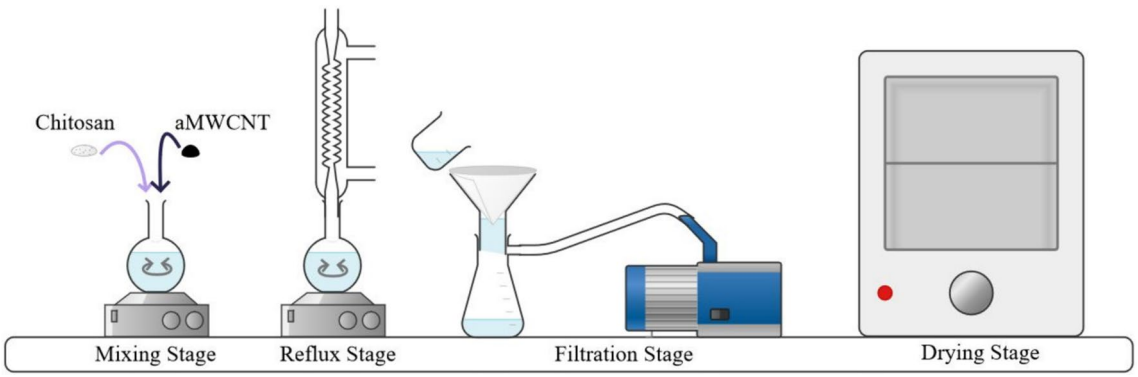

Fig. 2 Schematic representation of Chitosan Grafting of a-MWCNT

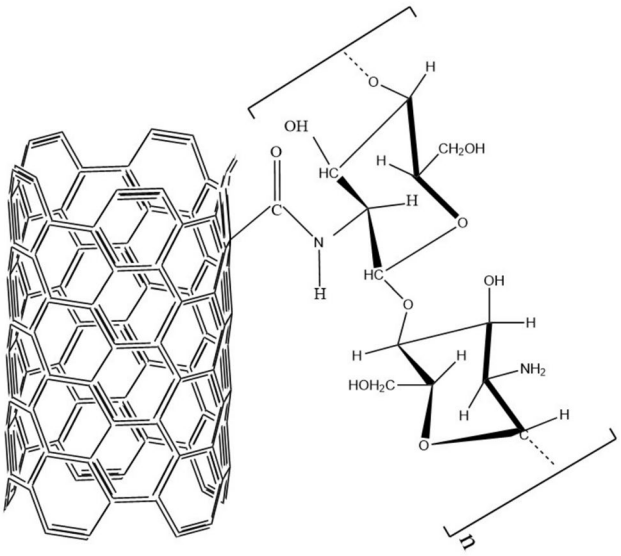

Fig. 3 Schematic representation of chitosan-grafted MWCNT

gas container cell ensures temperature and pressure stability before the gas enters the reaction cell.

The temperature and pressure were measured and controlled in the reaction cell every 10 s. Gas pressures in both cells were monitored using a digital pressure gauge with an accuracy of ± 0.25, capable of measuring pressures ranging from − 20 to 900 psia.

Initially, 100 g of feed was introduced into the reactor. Any residual air was evacuated from the system, and the gas container was pressurized to the desired CO_2 pressure. A temperature controller (accuracy: ± 0.2 °C) maintained the entire apparatus at a constant temperature. The gas remained in the container until it reached a stable pressure and temperature.

Subsequently, CO_2 was allowed to enter the reaction cell, initiating the absorption process. Continuous stirring was performed to enhance mass transfer and prevent particle accumulation during absorption. Temperature and pressure data were automatically collected by the temperature and pressure transducers.

Numbers of injected CO_2 mole to the absorption cell $\left(n^T_{CO_2}\right)$ and remained mole of it in the reactor $\left(n^g_{CO_2}\right)$ were calculated as follows (Park and Sandall 2001; Mondal et al. 2016):

$$n^T_{CO_2} = \frac{V_b}{RT}\left(\frac{P_{b_1}}{Z_1} - \frac{P_{b_2}}{Z_2}\right) \tag{1}$$

$$n^g_{CO_2} = \frac{V^g_c}{RT_f}\frac{P_{CO_2}}{Z_{CO_2}} \tag{2}$$

In this context, '1' and '2' represent the gas states in the container cell just before opening V-2 and after closing V-3, respectively. In Eq. (1), P (kPa), V_b (cm^3), T (K) and R represent the absolute pressure, the volume of the gas-containing

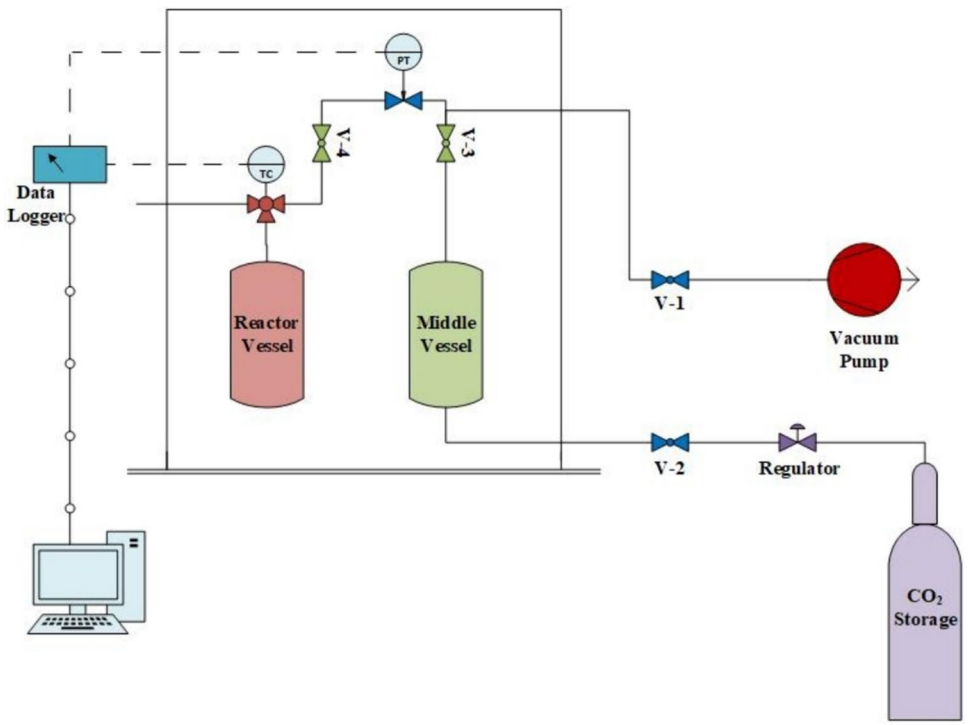

Fig. 4 Schematic diagram of CO_2 absorption setup

cell and its connecting pipes, the oven temperature, and the universal gas constant (8.314 J mole^{-1} K^{-1}), respectively.

In Eq. (2), P_{CO_2}, V_c^g, T_f denote the gas pressure in the equilibrium state (kPa), the volume of the reactor and its connections minus the liquid volume (cm^3), and the final solution temperature (K), respectively. The gas compressibility factors (Z) were estimated for the initial and final states of the container (Z_1, Z_2) and the final state of the reactor (Z_{CO_2}) using the Peng-Robinson equation of state.

The absorbed moles of CO_2 by the absorber (n_{CO_2}) are calculated by Eq. (3):

$$n_{CO_2} = n_{CO_2}^T - n_{CO_2}^g \tag{3}$$

The absorption capability of solutions is assessed by α (mole kg^{-1}) which is the absorbed mole of gas (n_{CO_2}) per kg of solution (0.1 kg) (Eq. 4):

$$\alpha = \frac{n_{CO_2}}{Kg(solution)} \tag{4}$$

Characterization of the sorbent

The modified MWCNTs were characterized using Fourier Transform Infrared Spectroscopy (FTIR), Scanning Electron Microscopy (SEM), and Organic Elemental Analysis (CHNS). FTIR spectroscopy was employed to confirm the successful attachment of functional groups during the amine-functionalization and polymer grafting processes. It also helped analyze the bonding types within the resulting particles.

SEM analysis was conducted to examine the surface morphology of the synthesized particles and compare it to the raw material. Additionally, CHNS elemental analysis enabled the measurement of the type and quantity of different elements present in the structures of aMWCNTs and gMWCNTs.

Results and discussion

Characterization of the sorbent

FTIR analysis

Figure 5 presents the FTIR spectra of chitosan, aMWCNT, and gMWCNT particles. Notably, a prominent peak within the 3434–3361 cm^{-1} range is evident in all three spectra, signifying the presence of –O–H stretching and intermolecular hydrogen bonds (Sassaki et al. 2015). The bands within the 1750–1550 cm^{-1} range represent C=O bending in aromatic rings and carboxyl groups of MWCNTs (Stobinski et al. 2010). The bands within 1300–950 cm^{-1} are ascribed to C–O bonds in various chemical surroundings (Stobinski

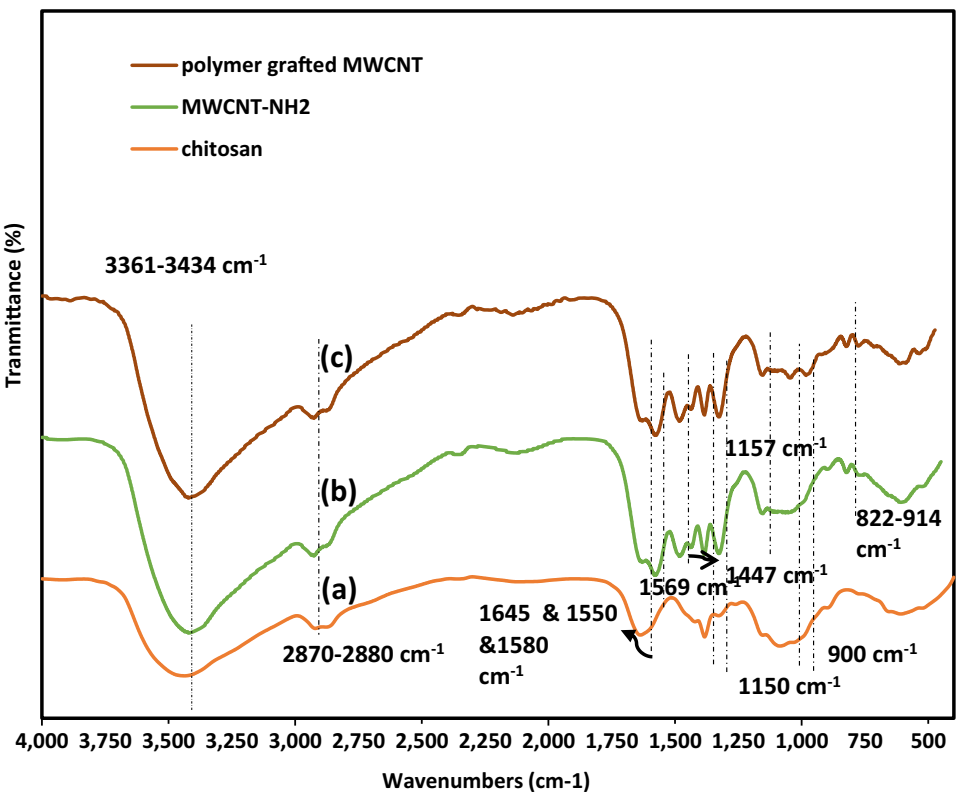

Fig. 5 Fourier transform infrared (FT-IR) spectroscopy of Chitosan (**a**), aMWCNT (**b**), and gMWCNT (**c**)

et al. 2010). In Fig. 5a and c, peaks at the 2880–2870 cm^{-1} region are assigned to C-H symmetric and asymmetric stretching in chitosan configuration. The wavenumbers 1154 and 1094 cm^{-1} are connected to C–O bending in the secondary alcohol of chitosan (Song et al. 2013). Furthermore, the bands at 897 cm^{-1} and 665 cm^{-1} are attributed to the C-H out-of-plane vibration and the N–H twist vibration in chitosan, respectively (Song et al. 2013). $–NH_2$ and –NH bends' frequencies in aMWCNT (Fig. 5b) can be associated with the 1570 and 1470 cm^{-1} bands (Liu and Shi 2014). The 1447 cm^{-1} frequency also affirms the formation of peptide bonds between MWCNTs' surface and amine groups in DAP (Lee et al. 2015). The gMWCNTs' spectrum (Fig. 5c) in the region of 3434–3361 cm^{-1} is intensified by –N–H bonds in the chitosan structure (Carson et al. 2009). Amide groups form as due to the reaction between carboxyl groups in multi-walled carbon nanotubes and amine groups of chitosan and DAP. Appeared peaks at 1645 cm^{-1} can be assigned to the C=O bond in amide I and at 1325 cm^{-1} to the C–N bond in amide III of the chitosan, respectively (Sassaki et al. 2015). Moreover, a small band at 1550 cm^{-1} can be ascribed to N–H bending of amide II in the chitosan polymer.

SEM analysis

SEM images in Fig. 6a, b, and c depict pristine MWCNTs, carboxylic MWCNTs, and aMWCNTs, respectively. The robust mechanical properties of MWCNTs preserved their morphology during carboxylation and amine functionalization.

In Fig. 6d, SEM images of chitosan-grafted MWCNTs are displayed, revealing a more amorphous nature and a rougher surface compared to carboxylic and amine-functionalized MWCNT particles (Fig. 6b and c). The presence of chitosan macromolecules is evident from the aggregation of impregnated molecules on the MWCNT surface.

CHN analysis

Table 1 shows the elemental analysis of amine-functionalized MWCNTs and chitosan-grafted MWCNTs. The increased percentage of N and H atoms in gMWCNT particles compared to aMWCNTs confirms that the chitosan groups have been successfully grafted on the surface of aMWCNT particles.

Effect of chitosan/aMWCNTs ratio on absorption performance

Figure 7 shows the CO_2 absorption capacity of nanofluids containing three synthesized samples with 1:1, 0.5:1 and 0.25:1 chitosan/aMWCNTs ratios at an initial pressure of 280 psi and temperature of 35 °C. Experiments intended to

Table 1 C, H and N content of aMWCNT and gMWCNT particles

Sample name	% C	% H	% N
aMWCNT	78.58	2.50	5.66
gMWCNT	71.52	4.27	7.78

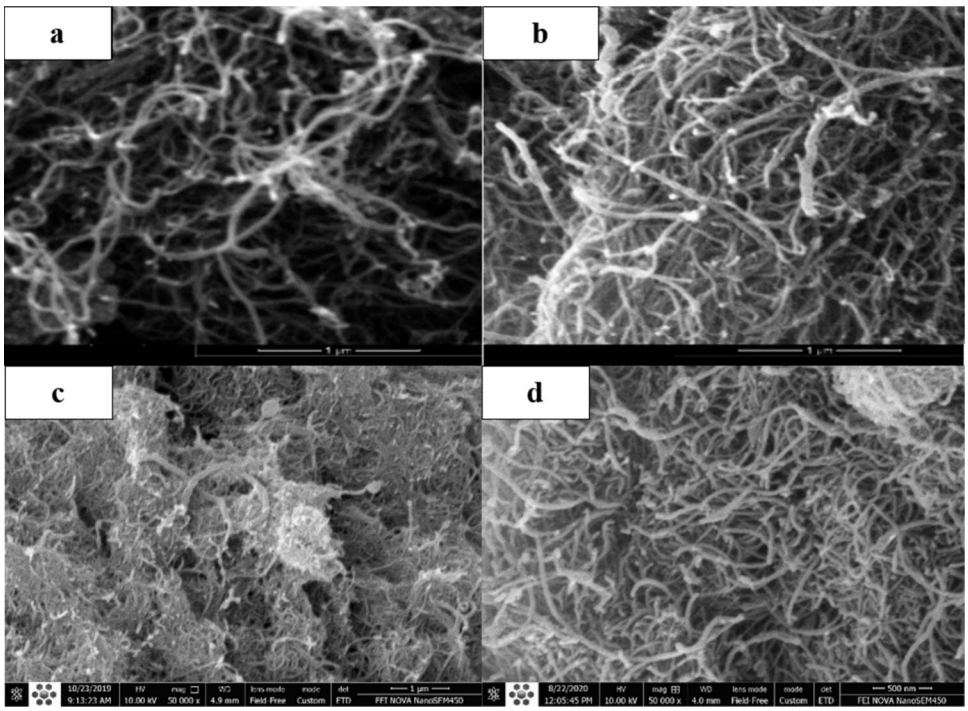

Fig. 6 SEM images of pristine MWCNT (**a**), Carboxylic MWCNT (**b**), aMWCNT (**c**), gMWCNT (**d**)

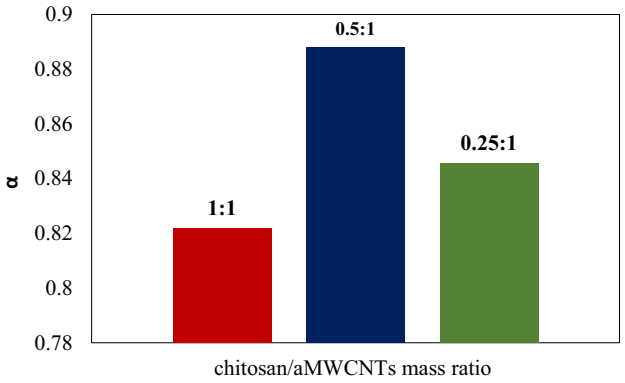

Fig. 7 CO_2 absorption amounts in MDEA-based (10 wt% MDEA) nanofluids containing three synthesized samples with 1:1, 0.5:1 and 0.25:1 chitosan/aMWCNTs ratio (initial pressure = 280 psi, T = 35 °C, stirrer rotation speed = 150 rpm)

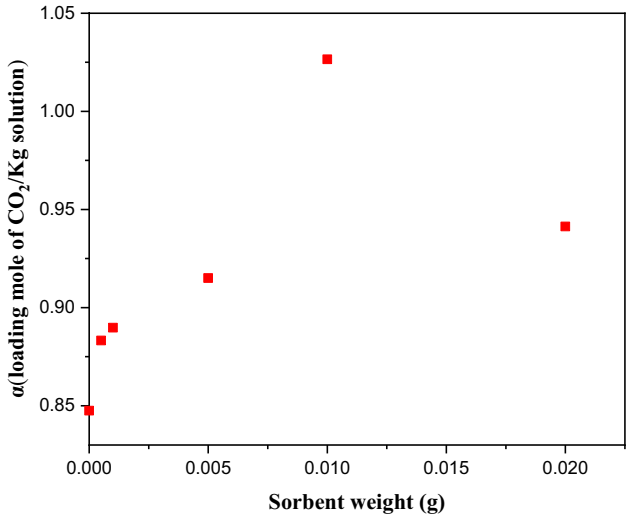

Fig. 8 CO_2 absorption amounts in MDEA-based (10 wt% MDEA) nanofluids containing 0.0005, 0.001, 0.005, 0.01 and 0.02 wt% of gMWCNTs (initial pressure = 280 psi, T = 35 °C, stirrer rotation speed = 150 rpm)

investigate the influence of the polymer's initial amount on the CO_2 absorption performance. As can be seen, the sample with 0.5:1 chitosan/aMWCNTs ratio exhibits superior CO_2 removal performance compared to samples with ratios of 1:1 and 0.25:1 in the synthesis process. In the ratio of 0.5:1 chitosan/aMWCNTs, the highest amount of absorbed CO_2 moles per kg of the solution was achieved (α value). Given the outstanding performance of the sample with 0.5:1 chitosan/aMWCNTs ratio under similar pressure and temperature conditions, this ratio was chosen for synthesizing a state-of-the-art sorbent which is signified as gMWCNT.

Effects of gMWCNTs concentration on absorption performance and kinetics

Figure 8 illustrates a quantitative comparison of CO_2 absorption performance in an amine-based Nanofluid with varying concentrations of gMWCNT (0.0005, 0.001, 0.005, 0.01, and 0.02 wt%) in 10 wt% aqueous MDEA solution. These measurements were conducted at a pressure of 280 psi and a temperature of 35 °C. As shown, with increasing the concentration of gMWCNT particles up to the optimum value of 0.01 wt%, the α amount (loading mole CO_2 per kg of solution) rises steadily and then falls afterwards. This behavior can be related to five proposed mass transfer mechanisms. First, there is a bubble-breaking effect proposed by Kim et al. (2008). It states that dispersed Nanoparticles cover CO_2 microbubbles, and as the dynamic energy of the solution improves owing to increased Nanoparticles' quantity, a higher rate of bubble cracking will be achieved (Pineda et al. 2012). As a result, the mass transfer area increases, and the gas diffusion into liquid bulk will be promoted (Kim et al. 2008). The second dominant model is the shuttle or grazing effect, proposed by Alper et al. (1980). In this mechanism, solid particles transfer gas molecules from the gas–liquid diffusion layer to the solution bulk (Alper et al. 1980). Hence, it has a refreshing effect on the gas–liquid interface, which multiplies with the rising number of solid particles (Alper et al. 1986). The third determining mechanism in nanoparticle mass transfer enhancement is the Brownian motion of dispersed particles that can trigger micro-convection inside the suspension (Krishnamurthy et al. 2006; Fang et al. 2014). Increasing the number of suspended particles can further improve micro-turbulence within the solution (Fang et al. 2014). Consequently, the mass transfer coefficient and gas absorption capacity will be enhanced (Fang et al. 2014). Finally, solid particles' collision and interaction in the diffusion layer will lead to a more turbulent and, at the same time, thinner gas–liquid interface (Kluytmans et al. 2003). This, in turn, induces a higher rate of gas diffusion into the liquid film (Kluytmans et al. 2003). In what is referred to as the 'hydrodynamic effect in gas–liquid boundary layer', an increase in particles' concentration can elevate collision probabilities and enhance mass transfer rate (Kluytmans et al. 2003). It is also worth noting that the rising number of amine-functionalized Nanoparticles enhances the likelihood of their chemical reaction with CO_2 molecules, thereby improving their removal capacity.

Despite the advantages of increasing the quantity of particles and enhancing gas removal capacity, they begin to hinder the absorption process after an optimal concentration. A further increase in the optimum concentration value decreases the average distance between particles and disrupts intermolecular forces. Consequently, suspension aggregation and sedimentation occur (Yu et al. 2012; Sharma and Mital 2016). Hence, increasing particle mass fraction will

jeopardize fluid stability and adversely affect gas solubility (Yu et al. 2012). At the same time, if the concentration passes a critical threshold, Brownian motion decreases due to the disruption in intermolecular interactions (Jung et al. 2012). Notably, a higher proportion of dispersed particles elevates solution viscosity, which hinders species' diffusion during absorption (Sundar et al. 2013). Importantly, an excess of nanoparticles in the host solvent hampers the effective interaction between the aqueous amine solution and CO_2 (Arshadi et al. 2019).

Regarding the experiments conducted on five mass fractions of gMWCNTs, a concentration of 0.01wt% was selected as the optimum concentration for subsequent tests.

Figure 9 depicts the variation of pressure difference with respect to the initial pressure versus time in an amine-based nanofluid with different concentrations of gMWCNT (0.0005, 0.001, 0.005, 0.01, and 0.02 wt%) in 10 wt% aqueous MDEA solution at 280 psi and 35 °C. As shown, the pressure value plummets to a roughly constant value in the first 2 h of the reaction period. This can be associated with the unsaturated nature of the nanofluid and its significant chemical driving force at the beginning of the reaction. In each of the five concentrations, changes in the pressure decrease in relation to the initial pressure versus time are downward; however, the figure has a steeper slope for 0.01 wt% concentration. Experiments demonstrate that the rate of pressure decreases in relation to initial pressure with time is slower for 0.001, 0.0005, 0.005, 0.02 and 0 wt%, respectively. The increased slopes of lines affirm that the presence of gMWCNTs has positively affected the absorption rate in comparison with neat amine fluid. This occurs due to the induced turbulence in the solution which is the direct result of particle interactions and collisions. The solution at the optimum concentration (0.01 wt%) exhibited a higher rate of absorption compared to aqueous MDEA 10 wt% solution and all other concentrations of gMWCNTs in a 2 h period.

CO_2 absorption experiments

After determining the optimal concentration of gMWCNT (0.01 wt%), experiments were pursued at 3 absorption temperatures (25, 35, and 45 °C). In each temperature, initial pressure was changed between 130 and 220 psi.

Figure 10 demonstrates the variation of α (loading mole of CO_2/kg of solution) versus final pressure at absorption temperatures of 25, 35, and 45 °C. As can be seen, absorption capacity is enhanced as the initial pressure increases. The positive effect of pressure on removal capacity can be attributed to the mounting driving force caused by rising the initial pressure.

As depicted, the α value decreased with rising temperature. This indicated that an increase in solution temperature hinders the gas removal process. Elevating the absorption temperature leads to an enhancement in the activation energy of the nanofluids due to more dynamic nanoparticles (Arshadi et al. 2019). Thus, more energetic Nanoparticles are more likely to undergo self-collisions, which ultimately results in their poorer removal performance (Arshadi et al. 2019).

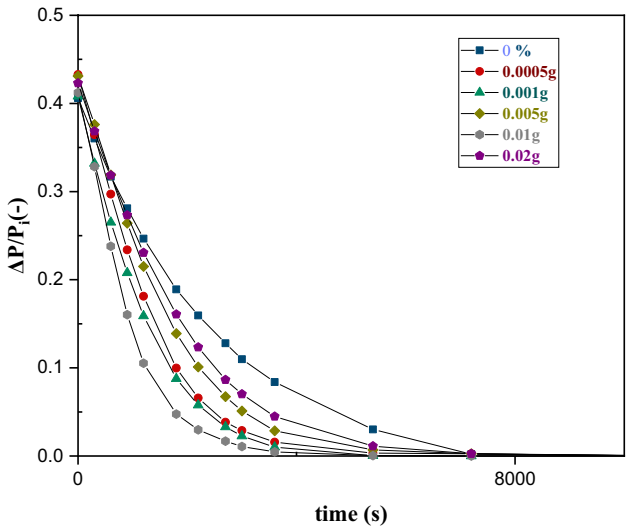

Fig. 9 Variation of pressure difference with respect to initial pressure by time in MDEA-based (10 wt% MDEA) nanofluids containing 0.0005, 0.001, 0.005, 0.01 and 0.02 wt% of gMWCNTs (initial pressure = 280 psi, T = 35 °C, stirrer rotation speed = 150 rpm)

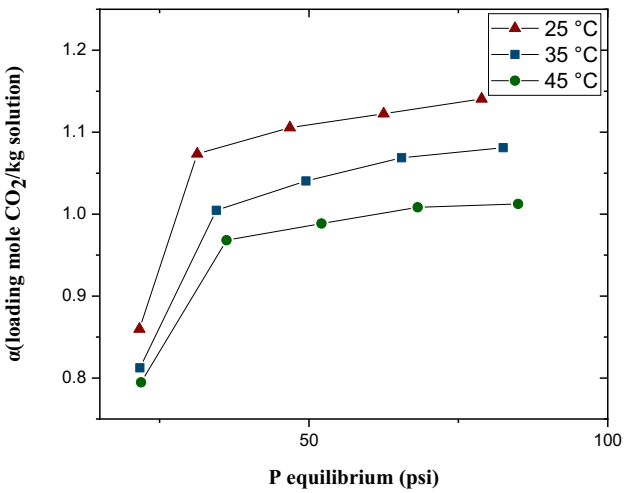

Fig. 10 Variation of CO_2 absorption amounts in MDEA-based (10 wt% MDEA) nanofluids containing the optimal concentration of gMWCNTs (T = 45 °C, stirrer rotation speed = 150 rpm)

Comparison between absorption performance of synthesized nanoparticles and neat solvent

Figure 11 compares the absorption enhancement observed in three samples: the neat solvent, a 10 wt% MDEA aqueous solution containing gMWCNTs, and a 10 wt% MDEA aqueous solution containing aMWCNTs. These tests were conducted at the optimal concentration of 0.01 wt% and temperature of 25 °C.

As depicted, the addition of synthesized nanoparticles improves absorption capacity. Specifically, the calculated enhancement is 12 and 20% higher than the aMWCNTs nanofluid and the neat solvent, respectively. In contrast, aMWCNT particles enhance the absorption capacity by a modest 8% compared to the fresh solvent. The results confirmed that gMWCNT particles could increase the removal efficiency compared to aMWCNTs in a 10 wt% MDEA aqueous solution, which can be attributed to two primary factors. Firstly, polymer impregnation enhances colloidal dispersibility and ensures a higher level of suspension stability, which results in superior removal of gas molecules during multiple absorption cycles. Sedimentation and clogging of nanoparticles would deteriorate nanofluid's attributes. According to mass transfer mechanisms, agglomeration and lack of stability in nanofluids, would decrease the gas absorption capability by bubble breaking effect, shuttle effect and Brownian motion. The formed clogs would also hinder sufficient collisions and interactions in the diffusion layer. The aMWCNT-containing solution, in comparison to the gMWCNT-containing solution, is more prone to settlement and agglomeration of its particles. As a result, during multiple experiments, aMWCNT-containing nanofluid exhibits mediocre absorption performance. In contrast, gMWCNT-containing solvent, which is a more stable and homogeneous solvent, would facilitate the absorption of CO_2 molecules and enhance gas removal efficiency. The second influential factor is that chitosan grafting may increase the likelihood of chemical adsorption of CO_2 molecules by the sorbent due to the abundance of amine groups in its structure.

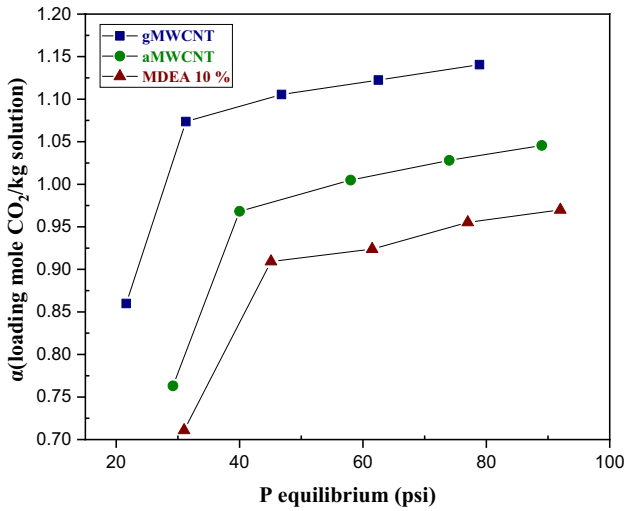

Fig. 11 CO_2 absorption improvement in MDEA-based (10 wt% MDEA) nanofluids in presence of 0.01 wt% gMWCNTs and 0.01 wt% aMWCNTs as opposed to neat solvent (T = 25 °C, stirrer rotation speed = 150 rpm)

Stability of amine-based nanofluids

This study pursued a higher level of colloidal stability in nanosuspensions. The dispersibility of amine-functionalized MWCNTs (aMWCNTs) and chitosan-grafted MWCNTs (gMWCNTs) in a 10 wt% MDEA aqueous solution was assessed by dissolving 0.01 g of synthesized nanoparticles in 100 g of solvent, followed by 45 min of sonication. Figure 12 depicts the behavior of aMWCNT-MDEA-water and gMWCNT-MDEA-water nanofluids immediately after preparation, 24 h later, and after one month of settling. Additionally, the stability of these nanofluids was further analyzed through zeta potential analysis.

As demonstrated in Fig. 12b, both prepared nanofluids exhibited commendable stability and uniformity after 24 h. Optical inspection of the samples, as shown in Fig. 12c, revealed that amine-functionalized MWCNT particles settled in the MDEA-based solution after one month, in contrast to chitosan-grafted MWCNT particles, which remained suspended. Therefore, chitosan-grafted MWCNTs exhibit improved long-term colloidal stability, owing to the additional presence of oxygen-containing functional groups (C=O, C–O) on the surface of the MWCNTs.

Zeta potential is the potential difference between the dispersion system and the stationary layer of bulk fluid, which is attached to suspended particles (Setia et al. 2013), which is a promising approach for assessing the durability of a stable suspension. It is worth noting that there is no specific absolute value of zeta potential that guarantees the long-term stability of nanofluids (Setia et al. 2013). Nevertheless, in accordance with various references, nanosuspensions with a zeta potential value exceeding 30 mV generally have satisfactory stability. Table 2 reveals the zeta potential value for MDEA-based nanofluids containing aMWCNTs and gMWCNTs. The measured zeta potential values for aMWCNT-MDEA-water and gMWCNT-MDEA-water nanofluids have been represented in the table which affirms the good stability of the gMWCNT-MDEA-water suspension.

Table 3 presents a comparison of prior research related to stability enhancement methods, focusing on the period during which water-based and MDEA-based nanofluids can maintain their stability. Owing to variations in sorbent

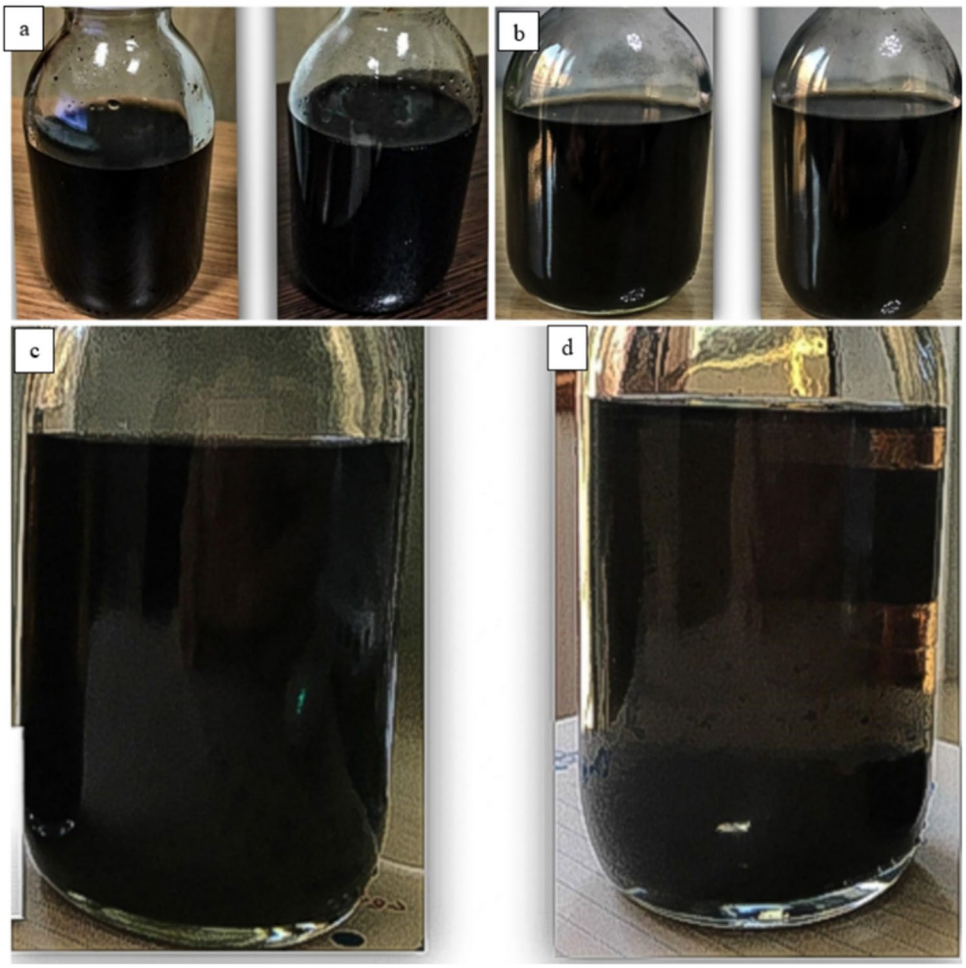

Fig. 12 Optical micrograph of gMWCNTs-MDEA-Water and aMWCNTs-MDEA-Water nanofluids (left to right) taken **a** right after preparation **b** 24 h after preparation **c** gMWCNTs-MDEA-Water one month after preparation. **d** aMWCNTs-MDEA-Water nanofluids one month after preparation

Table 2 Zeta potential of MDEA-based nanofluids containing aMWCNT and gMWCNT

Type of nanofluid	Zeta potential (mv)
aMWCNT-MDEA-H_2O	− 27/8
gMWCNT-MDEA-H_2O	− 34/5

characteristics and the base solvents across different studies, making an exact comparison can be challenging. However, unlike previous research, this study introduces a straightforward approach to extend the stability of nanofluids contained amine-functionalized MWCNT particles for one month. The achieved stability period in this study, surpasses the duration achieved in any other study in this field.

Table 3 Summary of nanofluids stability duration for different nanosorbents in water-based and MDEA-based solutions

Base particle	Solvent	Nanofluid stability improvement method	Stability duration	References
MWCNT	10 wt% aqueous MDEA	Graft of chitosan polymeric chains	One month	This study
Fe_3O_4	Water	Amine functionalization	After preparation and during experiments	Ha et al. (2022)
MWCNT	MDEA	Amine functionalization	60 min	Rahimi et al. (2020)
MWCNT	Pure water and MDEA	Adding surfactant	30 h	Baghery et al. (2019)
MWCNT	Ro water	Addition of Nitrogen functional groups (Decomposition of Nitrogen-rich Plasma Polymer Layer)	After preparation and during experiments	Jorge and Coulombe (2015)

Conclusion

The primary objective of this study was to address the issue of agglomeration in nanofluids containing multi-walled carbon nanotubes (MWCNTs) modified with amine groups and polymer configurations. Additionally, The CO_2 absorption capacities of these nanofluids were measured and compared. The hydrophobic nature of MWCNTs was modified through acid treatment, followed by the introduction of amine groups onto the carboxylic MWCNTs' surfaces, resulting in a product referred to as aMWCNT. In the subsequent step, chitosan chains, rich in amine and hydrophilic functional groups, were linked to the surface of aMWCNTs. The chitosan grafting process was performed using three polymer/MWCNTs ratios (1:1, 0.5:1, and 0.25:1), with a 0.5:1 ratio (gMWCNTs) selected as the optimal synthesis ratio for CO_2 absorption capacity. The successful development of amine groups and chitosan chains was confirmed through FTIR, SEM, and CHNS analysis. The principal aim of our research was to achieve a higher level of suspension stability by incorporating chitosan chains. This enhanced stability in gMWCNTs-MDEA-water solutions compared to aMWCNTs-MDEA-water solutions was corroborated through zeta potential analysis and optical inspection of the solvent over one month. To attain the second objective of this study, absorption measurements were conducted on various mass fractions (0.0005, 0.001, 0.005, 0.01 and 0.02 wt%) of gMWCNTs and 0.01 wt% concentration exhibited highest CO_2 uptake in a specific pressure and temperature. In the second step, the variation of α (loading mole CO_2 per kg of solution) was studied at three absorption temperatures (25, 35, and 45 °C). The CO_2 absorption capacity of the neat solvent was compared with that of solvents containing aMWCNTs and gMWCNTs, respectively. The results showed that gMWCNTs-MDEA-water solutions exhibited a significant increase in CO_2 uptake, with enhancements of 12 and 20% compared to aMWCNTs-MDEA-water solutions and the aqueous MDEA solution (10 wt%), respectively. However, the improvement in CO_2 uptake for aMWCNTs-MDEA-water solutions compared to the neat amine solution was only marginal, approximately 8%.

Acknowledgements The authors wish to thank all who assisted in conducting this work.

Author contributions Samaneh Sadeddin: Validation, Formal analysis, Investigation, Data Curation, Writing-Original draft, visualization; Mojgan Abbasi: Conceptualization, Methodology, Validation, Resources, Writing—Review & Editing, Supervision; Siavash Riahi: Conceptualization, Resources, Supervision, Project administration, Writing—Review & Editing, Funding acquisition.

Declarations

Conflict of interest The authors have no competing interests to declare that are relevant to the content of this article.

References

Agarwal P, Qi H, Archer LA (2010) The ages in a self-suspended nanoparticle liquid. Nano Lett 10:111–115. https://doi.org/10.1021/nl9029847

Alper E, Öztürk S (1986) The effect of activated carbon loading on oxygen absorption into aqueous sodium sulphide solutions in a slurry reactor. Chem Eng J 32:127–130

Alper E, Wichtendahl B, Deckwer W-D (1980) Gas absorption mechanism in catalytic slurry reactors. Chem Eng Sci 35:217–222

Arshadi M, Taghvaei H, Abdolmaleki MK et al (2019) Carbon dioxide absorption in water/nano fl uid by a symmetric amine-based nanodendritic adsorbent. Appl Energy 242:1562–1572. https://doi.org/10.1016/j.apenergy.2019.03.105

Baghery R, Riahi S, Abbasi M, Mohammadi-khanaposhtani M (2019) Investigation of the CO_2 absorption in pure water and MDEA aqueous solution including amine functionalized multi-wall carbon nano tubes. J Mol Liq 293:111431. https://doi.org/10.1016/j.molliq.2019.111431

Basheer BV, Jacob J, Siengchin S (2020) Polymer grafted carbon nanotubes—synthesis, properties, and applications : a review. Nano Struct Nano Objects 22:100429. https://doi.org/10.1016/j.nanoso.2020.100429

Breuer O, Sundararaj U (2004) Big returns from small fibers: a review of polymer/carbon nanotube composites. Polym Compos 25:630–645. https://doi.org/10.1002/pc.20058

Carson L et al (2009) Synthesis and characterization of chitosan–carbon nanotube composites. Mater Lett 63(6–7):617–620

Cui M, Chen S, Qi T, Zhang Y (2018) Investigation of CO_2 capture in nonaqueous ethylethanolamine solution mixed with porous solids. J Chem Eng Data. https://doi.org/10.1021/acs.jced.7b00761

Fang X, Xuan Y, Li Q et al (2014) Experimental investigation on enhanced mass transfer in nanofluids. Appl Phys Lett 203108:2007–2010. https://doi.org/10.1063/1.3263731

Figueroa D, Fout T, Plasynski S et al (2008) Advances in CO_2 capture technology—the US Department of Energy's Carbon Sequestration Program. Int J Greenh Gas Control 2:9–20. https://doi.org/10.1016/S1750-5836(07)00094-1

Golkhar A, Keshavarz P, Mowla D (2013) Investigation of CO_2 removal by silica and CNT nanofluids in microporous hollow fiber membrane contactors. J Memb Sci 433:17–24. https://doi.org/10.1016/j.memsci.2013.01.022

Gür TM (2022) Carbon dioxide emissions, capture, storage and utilization: review of materials, processes and technologies. Prog Energy Combust Sci 89:100965. https://doi.org/10.1016/j.pecs.2021.100965

Ha J, Won J, Ahn H, Tae Y (2022) Development of novel nanoabsorbents by amine functionalization of Fe_3O_4 with intermediate ascorbic acid coating for CO_2 capture enhancement. J CO2 Util 65:102228. https://doi.org/10.1016/j.jcou.2022.102228

Hsan N, Dutta PK, Kumar S et al (2020) Capture and chemical fi xation of carbon dioxide by chitosan grafted multi- walled carbon nanotubes. J CO2 Util 41:101237. https://doi.org/10.1016/j.jcou.2020.101237

Irani V, Tavasoli A, Maleki A, Vahidi M (2018) Polyethyleneimine-functionalized HKUST-1/MDEA nanofluid to enhance the absorption of CO_2 in gas sweetening process. Int J Hydrog Energy 43:5610–5619. https://doi.org/10.1016/j.ijhydene.2018.01.120

Ismail AF, Goh PS, Tee JC et al (2008) A review of purification techniques for carbon nanotubes. NANO 03:127–143. https://doi.org/10.1142/S1793292008000927

Jorge L, Coulombe S (2015) Nanofluids containing MWCNTs coated with nitrogen-rich plasma polymer films for CO_2 absorption in aqueous medium. Plasma Process Polym 12:1311–1321. https://doi.org/10.1002/ppap.201500040

Jung J, Lee JW, Kang YT (2012) CO_2 absorption characteristics of nanoparticle suspensions in methanol. J Mech Sci Technol 26:2285–2290. https://doi.org/10.1007/s12206-012-0609-y

Khaheshi S, Riahi S, Mohammadi-Khanaposhtani M, Shokrollahzadeh H (2019) Prediction of amines capacity for carbon dioxide absorption based on structural characteristics. Ind Eng Chem Res 58:8763–8771. https://doi.org/10.1021/acs.iecr.9b00567

Khodadadi MJ, Abbasi M, Riahi S, Shokrollahzadeh H (2019) Investigation on kinetics of carbon dioxide absorption in aqueous solutions of monoethanolamine+ 1, 3-diaminopropane. Sep Sci Technol 54:2800–2808. https://doi.org/10.1080/01496395.2018.1553984

Kim SH, Kim WG, Kang HU, Jung KM (2008) Synthesis of silica nanofluid and application to CO_2 absorption. Sep Sci Technol 43:3036–3055. https://doi.org/10.1080/01496390802063804

Kluytmans JHJ, Van WBGM, Kuster BFM, Schouten JC (2003) Mass transfer in sparged and stirred reactors: influence of carbon particles and electrolyte. Chem Eng Sci 58:4719–4728. https://doi.org/10.1016/j.ces.2003.05.004

Krishnamurthy S, Bhattacharya P, Phelan PE, Prasher RS (2006) Enhanced mass transport in nanofluids. Nano Lett 6:419–423. https://doi.org/10.1021/nl0522532

Kumar S, e Silva JD, Wani MY et al (2017) Carbon dioxide capture and conversion by an environmentally friendly chitosan based meso-tetrakis(4-sulfonatophenyl) porphyrin. Carbohydr Polym 175:575–583. https://doi.org/10.1016/j.carbpol.2017.08.031

Lee M, Lee S, Park S (2015) Preparation and characterization of multi-walled carbon nanotubes impregnated with polyethyleneimine for carbon dioxide capture. Int J Hydrog Energy 40:3415–3421. https://doi.org/10.1016/j.ijhydene.2014.12.104

Li P, Yang R, Zheng Y et al (2015) Effect of polyether amine canopy structure on carbon dioxide uptake of solvent-free nano fluids based on multiwalled carbon nanotubes. Carbon 95:408–418. https://doi.org/10.1016/j.carbon.2015.08.060

Liu Q, Shi Y (2014) Amine-functionalized low-cost industrial grade multi-walled carbon nanotubes for the capture of carbon dioxide. J Energy Chem 23:111–118. https://doi.org/10.1016/S2095-4956(14)60124-8

Liu Z, Rong F, Yuying Y (2022) Preparation and evaluation of stable nanofluids for heat transfer application. Advances in nanofluid heat transfer. Elsevier, Amsterdam, pp 25–57

Masuko T, Minami A, Iwasaki N et al (2005) Thiolation of chitosan. Attachment of proteins via thioether formation. Biomacromol 6:880–884. https://doi.org/10.1021/bm049352e

Mondal BK, Bandyopadhyay SS, Samanta AN (2016) Equilibrium solubility measurement and Kent-Eisenberg modeling of CO_2 and hexamethylenediamine. Greenh Gases Sci Technol 13:1–13. https://doi.org/10.1002/ghg

Nabipour M, Keshavarz P, Raeissi S (2017) Experimental investigation on CO_2 absorption in Sulfinol-M based Fe_3O_4 and MWCNT nanofluids. Int J Refrig 73:1–10. https://doi.org/10.1016/j.ijrefrig.2016.09.010

Ngoy JM, Wagner N, Riboldi L, Bolland O (2014) A CO_2 capture technology using multi-walled carbon nanotubes with polyaspartamide surfactant. Energy Procedia 63:2230–2248. https://doi.org/10.1016/j.egypro.2014.11.242

Pahija E, Golshan S, Blais B, Boffito DC (2022) Perspectives on the process intensification of CO_2 capture and utilization. Chem Eng Process Process Intensif 176:108958. https://doi.org/10.1016/j.cep.2022.108958

Park MK, Sandall OC (2001) Solubility of carbon dioxide and nitrous oxide in 50 mass methyldiethanolamine. J Chem Eng Data 46:166–168

Peniche C, Argüelles-Monal W, Peniche H, Acosta N (2003) Chitosan: an attractive biocompatible polymer for microencapsulation. Macromol Biosci 3:511–520. https://doi.org/10.1002/mabi.200300019

Pineda IT, Lee JW, Jung I et al (2012) CO_2 absorption enhancement by methanol-based Al_2O_3 and SiO_2 nanofluids in a tray column absorber. Int J Refrig 35:1402–1409. https://doi.org/10.1016/j.ijrefrig.2012.03.017

Rahimi K, Riahi S, Abbasi M (2020) Effect of host fluid and hydrophilicity of multi-walled carbon nanotubes on stability and CO_2 absorption of amine-based and water-based nanofluids. J Environ Chem Eng 8:103580. https://doi.org/10.1016/j.jece.2019.103580

Saidi M (2020) CO_2 absorption intensification using novel DEAB amine-based nano fluids of CNT and SiO_2 in membrane contactor. Chem Eng Process Process Intensif 149:107848. https://doi.org/10.1016/j.cep.2020.107848

Sassaki GL, Alexandre H, Rocha O (2015) Does the use of chitosan contribute to oxalate kidney stone formation. Mar Drugs 13:141–158. https://doi.org/10.3390/md13010141

Setia H, Gupta R, Wanchoo RK (2013) Stability of nanofluids. Materials science forum, vol 757. Trans Tech Publications Ltd., Freienbach, pp 139–149

Sharma SK, Mital S (2016) Preparation and evaluation of stable nanofluids for heat transfer application: a review. Exp Therm Fluid Sci 79:202–212. https://doi.org/10.1016/j.expthermflusci.2016.06.029

Smith B, Wepasnick K, Schrote KE et al (2009) Colloidal properties of aqueous suspensions of acid-treated, multi-walled carbon nanotubes. Environ Sci Technol 43:819–825. https://doi.org/10.1021/es802011e

Song C, Yu H, Zhang M et al (2013) Physicochemical properties and antioxidant activity of chitosan from the blowfly *Chrysomya megacephala* larvae. Int J Biol Macromol 60:347–354. https://doi.org/10.1016/j.ijbiomac.2013.05.039

Spitalsky Z, Tasis D, Papagelis K et al (2010) Carbon nanotube–polymer composites: chemistry, processing, mechanical and electrical properties. Prog Polym Sci 35(3):357–401

Stobinski L, Lesiak B, Kövér L et al (2010) Multiwall carbon nanotubes purification and oxidation by nitric acid studied by the FTIR and electron spectroscopy methods. J Alloys Compd 501:77–84. https://doi.org/10.1016/j.jallcom.2010.04.032

Sundar LS, Sharma KV, Naik MT, Singh MK (2013) Empirical and theoretical correlations on viscosity of nanofluids: a review. Renew Sustain Energy Rev 25:670–686. https://doi.org/10.1016/j.rser.2013.04.003

Tsubokawa N (2011) Grafting of polymers onto carbon nanotubes. Nippon Gomu Kyokaishi 83:361–366

Urmi WT, Rahman MM, Kadirgama K et al (2020) An overview on synthesis, stability, opportunities and challenges of nanofluids. Mater Today Proc 41:30–37. https://doi.org/10.1016/j.matpr.2020.10.998

Vaisman L, Marom G, Wagner HD (2006) Dispersions of surface-modified carbon nanotubes in water-soluble and water-insoluble polymers. Adv Funct Mater 16:357–363. https://doi.org/10.1002/adfm.200500142

Weiland RH, Hatcher NA, Nava JL (2010a) Post-combustion CO_2 capture with amino-acid salts. GPA Eur 22:24

Wepasnick KA, Smith BA, Bitter JL, Fairbrother DH (2010b) Chemical and structural characterization of carbon nanotube surfaces. Anal Bioanal Chem 396:1001–1014. https://doi.org/10.1007/s00216-009-3332-5

Wepasnick KA, Smith BA, Schrote KE et al (2011) Surface and structural characterization of multi-walled carbon nanotubes following different oxidative treatments. Carbon 49:24–36. https://doi.org/10.1016/j.carbon.2010.08.034

Yu H, Hermann S, Schulz SE et al (2012) Optimizing sonication parameters for dispersion of single-walled carbon nanotubes. Chem Phys 408:11–16. https://doi.org/10.1016/j.chemphys.2012.08.020

Yu W, Wang T, Park AHA, Fang M (2019) Review of liquid nano-absorbents for enhanced CO_2 capture. Nanoscale 11(37):17137–17156